An Efficient Approach towards Thunderstorm Detection Using Saliency Map

Rasika P. Gawande[1], Prof. Namrata D. Ghuse[2]

Department of computer science and engineering,
S.G.B.A. University,
Amravati, India.

Abstract— **Thunderstorm is a sudden electrical expulsion manifested by a lightening with a particular sound. It is one of the most spectacular weather phenomena in the atmosphere which occurs seasonally. The prediction of thunderstorms is said to be the most complicated task in weather forecasting, due to its spatial and temporal extension either dynamically or physically. Every thunderstorm produce lightening, this kills more people every year than tornadoes and hurricanes. Heavy rain from thunderstorm leads to flooding and causes extensive loss to property and other living organisms. Different scientific, technological researches are been carried on the forecasting of this severe weather feature in advance to reduce damages. In this, many of the researchers proposed various methodologies like TOA Method, DF+TOA method, Interferometry method, and segmentation based method and so on for the detection. The research work adopted clustering and wavelet transform techniques in order to improve the thunderstorm prediction rate. The study carried on the thunderstorm prediction using saliency map, clustering and wavelet techniques resulting with higher accuracy.**

Keywords- **Clustering, Haar wavelet transform, Saliency map, Satellite imagery, Thunderstorm.**

I. INTRODUCTION

A thunderstorm is a rain shower during which you hear thunder sound and thunder. Since thunder comes from lightning, all thunderstorms have lightning. Three basic ingredients are required for a thunderstorm to form i.e. moisture, unstable air, and a lifting mechanism to provide the "nudge." The sun heats the surface of the earth and warms the air above the surface of the earth. If this warm surface air is forced to rise—hills or mountains, or areas where warm and cold or wet and dry air bump together can cause rising motion—it will continue to rise as long as it weighs less and stays warmer than the air around it. Then the air rises, it transfers heat from the surface of the earth to the upper levels of the atmosphere. The water vapour starts begins to cooled, releases the heat, condenses and forms the cloud. The cloud grows upward into areas where the temperature is cooled. As a storm rises to the cooled region, different types of ice particles can be created from freezing water drops. The particles can grow by condensing vapour like frost and by collecting smaller liquid drops that haven't frozen yet (a state called "super cooled"). When two cooled particles collide, they collide with each other, but one particle can rip off a little bit of ice from the other one and grab some electric charge. Lots of this collision can build

up big regions of electric charges to cause a lightning, which creates the sound waves hear as thunder.

Thunderstorms have three stages in their life cycle: The developing stage, the maturity stage, and the dissolving stage. In the developing stage of a thunderstorm, it is marked by a cumulus cloud that is being pushed upward by a rising column of air (updraft). The cumulus cloud soon looks like a tower (called towering cumulus) as the updraft continues to develop. There is no rain during this stage but occasional cause lightning. Then thunderstorm enters into the maturity stage. When the updraft continues to feed the storm, but the precipitation begins to fall out of the storm, creating a downdraft (a column of air pushing downward). When the downdraft and the cooled air spread out along the ground it forms a gust front, or a line of gusty winds. The maturity stage is the most likely for heavy rain, lightning, strong winds, and tornadoes. Then a large amount of precipitation is produced and the updraft is overcome by the downdraft beginning in the dissolving stage. At the ground, the gust moves out a long distance from the storm and cuts off the warm and moist air that was feeding the thunderstorm. Then rainfall decreases in intensity, but lightning remains a dangerous.

II. LITERATURE SURVEY

Watson-Watt and Herd [13] in 1920 developed a cathode-ray direction finder (CRDF) that utilized a pair of orthogonal loop antennas tuned to a frequency near 10 kHz, where propagation in the earth- ionosphere waveguide is relatively efficient to detect the horizontal magnetic field produced by lightning. The angle to the discharge was obtained by displaying the north-south and east- west antenna outputs simultaneously on an x-y oscilloscope, so that the resulting vector pointed in the direction of the discharge. Two or more CRDFs at known positions were sufficient to determine the location of a discharge from the intersection of simultaneous direction vectors. Various low frequency CRDF systems were used up to and during World War II in many regions of the world.

Lewis et al. [7] in 1960 have described a method for locating lightning that is based on measurements of the time-of-arrival of a radio pulse at several stations that are precisely synchronized. A constant difference in the arrival time at two stations defines a hyperbola, and multiple stations provide multiple whose intersections define a source location. Time- of-arrival (TOA) methods can provide accurate locations at long ranges.

E. P. Krider, R. C. Noggle, and M. A. Uman in 1976 an improved magnetic DF system was developed for locating cloud-to-ground lightning within a range of about 500 km. This system operated in the time-domain (i.e., covering the LF and VLF bands from about 1 to 500 kHz) and was designed to respond to field waveforms that were characteristic of the return strokes in CG flashes [6]. When such a field was detected, the magnetic direction was sampled (in both a north-south loop and an east-west loop) just at the time of the initial field peak. The resulting direction vector pointed as closely as possible to the onset of the stroke and to the place where the stroke struck ground.

Hayenga and Warwick [5] in 1981 showed that a radio interferometer could be used to measure the azimuth and elevation angles of lightning sources at VHF frequencies. Rhodes et al. and Shao et al. have developed this technique and have used single-station interferometers to improve our understanding of the development of both IC and CG lightning. These were single station systems that provide a "projection" of lightning onto a plane. Richard et al., and have developed multiple-station networks of interferometers that can locate and map the sources of VHF radiation in two- or three-dimensions with high time resolution.

J.A. Cramer, K.L. Cummins[10] in 1989, they are capable of detecting VLF "spherics" produced by very distant cloud-to- ground lightning. These signals propagate thousands of kilometres by ionospheric reflection. Standard LF/VLF sensors can be simultaneously employed for their conventional use and for this long-range application. For this long-range application, the sensor information is processed in a manner that identifies and employs ionospherically-propagated electromagnetic signals produced by distant lightning, rather than the "normal" ground-wave propagated signals.

Casper and Bent [11] in 1992 have developed a wideband TOA receiver (termed the Lightning Position and Tracking System or LPATS) that is suitable for locating lightning sources at medium and long ranges using the hyperbolic method.

K.L. Cummins, R.O. Burnett, W.L. Hiscox and A.E. Pifer [12] in 1993, Global Atmospherics developed a method for combining direction-finding and time-of-arrival to produce yet another lightning location method which we refer to as the IMPACT method. In this approach, direction finding provides azimuth information and absolute arrival time provides range information. These measurements produce three parameters -- latitude, longitude, and discharge time. Thus, IMPACT method has redundant information which allows for an optimized estimate of location even when only two sensors provide both timing and angle information.

L. Maier, C. Lennon, T. Britt, and S. Schaefer in 1995, the NASA Kennedy Space Center has developed a Lightning Detection and Ranging (LDAR) System that is capable of providing three-dimensional locations of more than a thousand RF pulses within each lightning flash [13], [33]. This system is similar to that of Proctor, but the data acquisition is automatic, and the data displays are generated in real-time. In order to facilitate the support of this system, which had been the only one of its kind, NASA entered into a technology transfer agreement with GAI to build a COTS version of the system in 1997.

Kishor Kumar Reddy, Anisha P R, Narasimha Prasad L V presented the work in 2014. It uses the segmentation based on clustering. An efficient technique to segment the input image into several clusters based on similarity measure; here Euclidean distance is used as one of the similarity metric. Here, Segmentation is performed to image by based on various color factors because colors possess wavelength values. The image containing relatively similar wavelength values are grouped into different clusters [14].
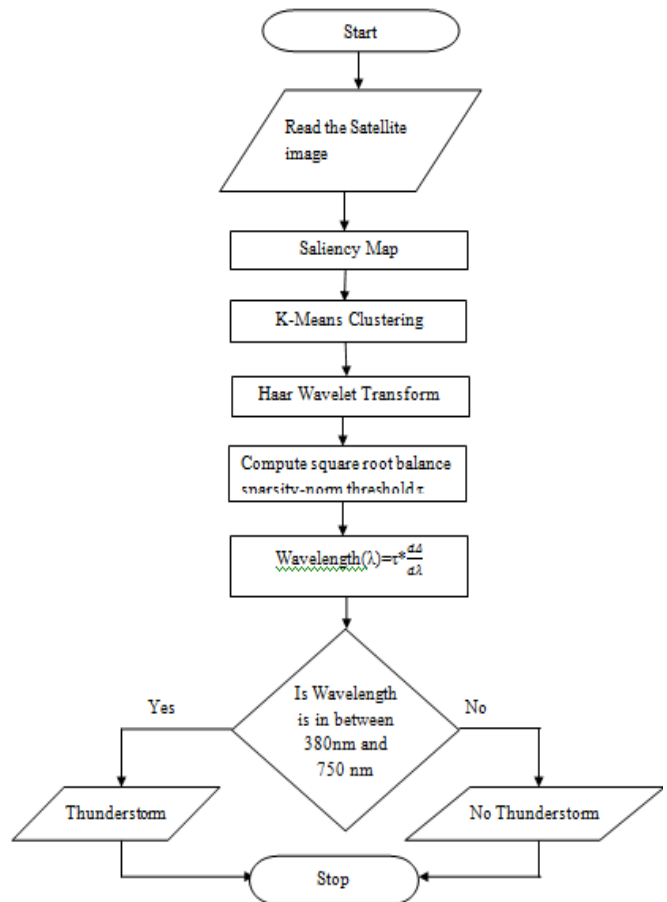
III. PROPOSED METHODOLOGY

Figure 1: Thunderstorm Detection flow chart

The proposed work divided into four parts,

A. Image Collection

The satellite imagery is viewable and the raw data archive can be taken from the US National Oceanic and Atmospheric Administration (NOAA)[16].

B. Saliency Map

First of all need the image which is pick up from the file and read the image form file with the help of read instruction. After reading the image, need to find the size of the image and also the rows, columns and number of colors. Then plot the image into the proper size as 256*256 pixels for further processing. Now, have proper size original image and the original image having the some energy

portion. The area of image having energy portion can be divided into the two parts i.e. the high energy portion is called foreground and the low energy portion is called background and need to find the foreground energy portion for that different methods can be applied as follows.

On the original image apply the saliency map method. In this saliency map the required data can be extracted on the basis of color, intensity, orientation, size, motion, depth, people and context. The intensity of an image can be calculated with the help of centre and surrounding of an image. Before applying the intensity factor some pre-processing parameters has been calculated and original image with red, green and blue channels Intensity as,

$$I = (r + g + b)/3$$

Broadly tuned color channels,

$$R = r - (g + b)/2$$

$$G = g - (r + b)/2$$

$$B = b - (r + g)/2$$

$$Y = (r + g)/2 - |r - g|/2 - b$$

The intensity of an image can be calculated with intensity of centre and surrounding and can be formulated as,

$$I(c, s) = | I(c) \ Q \ I(s)|$$

And then the color feature can be extracted as,

$$RG(c, s) = | (R(c) - G(c)) \ Q \ (G(s) - R(s)) |$$

$$BY(c, s) = | (B(c) - Y(c)) \ Q \ (Y(s) - B(s)) |$$

Same c and s as with intensity. Then apply the third feature i.e. orientation feature. In this orientation feature, on the different angle the image can be calculated for that need to create Gabor pyramids for the angles,
For q = {0º, 45º, 90º, 135º}

$$O(c, s, \theta) = |O(c, \theta) - O(s, \theta)|$$

After getting saliency map image, get the energy part of the image then apply the quaternion method, the quaternion method is the method which is help in getting the energy of the each pixel. The pixel calculation can be done by performing the matrix calculation by comparing a pixel in the 3D space with another pixel. Now, apply the Gaussian filter in a loop of 1 to 8 scale to the Gaussian filter so that after every iteration will get the some more portion of the energy and smooth image. The Gaussian smoothing operator performs a weighted average of surrounding pixels based on the Gaussian distribution. It is used to remove Gaussian noise and is a realistic model of defocused lens.

C. K- Means Clustering

The saliency map image gets from the first part. Now, apply K-means clustering algorithm to the saliency map image. K-means clustering is a well known partitioning method. In this objects are classified as belonging to one of K-groups. The results of partitioning method are a set of K clusters, each object of data set belonging to one cluster. In each cluster there may be a centroid or a cluster representative. In case where we consider real-valued data, the arithmetic mean of the attribute vectors for all objects within a cluster provides an appropriate representative.
Algorithm for K-means clustering:-
1. Start
2. Take the saliency map image.
3. Split an Image into multi cluster.
4. Assign each pixel in the image to cluster to minimize distance between pixel and cluster centroid.
5. Re-compute the clusters by averaging all of the pixels in the centroid.
6. Repeat the step 2 and step 3 until no pixel change cluster.
7. Stop

D. Haar Wavelet Transformation

Haar Wavelet compression is an efficient way to perform both lossless and loosely compression. It relies on averaging and differencing values in an image matrix to produce a matrix which is sparse or nearly sparse. After applying the thresholding method, it helps in getting the threshold value of wavelength calculation. Now, will have the detected region and want the values for the calculation of the wavelength for that assign some parameters i.e. a for approximate value ,h for horizontal, v for vertical, d for diagonal values of the image. All these values helps in the calculating the standard deviation (σ) value. The 'n' is length, it is calculated from standard deviation i.e. the value of the standard deviation is greater than 0 that is the value of n. Then threshold value is calculated as,

$$\tau = \sqrt{\frac{2\sigma^2 \log(n)}{n}}$$

Fixed threshold value is calculated by,

$$\tau_R = \int_0^{255} (\frac{dA}{dA} \ \sqrt{\frac{2\sigma^2 \log(n)}{n}}) dn$$

Now, Wavelength factor value is to be computed as,

$$\text{Wavelength } (\lambda) = \tau * \frac{dA}{dA}$$

IV. RESULT ANALYSIS

The satellite imagery is publicly viewable and the raw data archive can be requested on the website of US National Oceanic and Atmospheric Administration (NOAA)[16]. It is analysed to identify the presence of thunderstorms within the clouds. On analysis of these satellite images, a threshold value is computed. As satellite image is a visible spectrum, its wavelength value always lies in the range of 380nm-750nm.

TABLE I: Experimental calculation for thunderstorm

Image No	Standard Deviation (σ)	Threshold Value (τ)	Wavelength (λ)= τ * $\frac{d\lambda}{d\tau}$
Image1.jpg	109.9055	9.0984	409.93
Image2.jpg	145.8404	14.7057	750.00
Image3.jpg	186.9235	12.6184	750
Image4.jpg	107.5160	9.8428	433.83
Image5.jpg	172.8464	17.8841	750
Image6.jpg	155.9906	14.4860	750
Image7.jpg	134.5546	9.2690	511.28
Image8.jpg	141.4751	11.8832	689.20
Image9.jpg	141.4751	11.8832	689.20
Image10.jpg	123.5159	8.7320	442.15
Image11.jpg	207.7356	15.3390	750
Image12.jpg	155.0245	9.6974	616.29
Image13.jpg	191.1254	11.5570	750
Image14.jpg	191.1254	11.5570	750
Image15.jpg	147.7022	8.8944	750
Image16.jpg	171.7789	17.2228	750
Image17.jpg	194.7903	9.8026	750
Image18.jpg	136.9136	7.6109	427.18
Image19.jpg	135.3804	8.5973	477.14
Image20.jpg	219.6878	18.4123	750
Image21.jpg	181.4343	8.6776	645.43
Image22.jpg	237.9543	20.9191	750
Image23.jpg	210.5246	10.9992	750
Image24.jpg	145.8866	10.5618	631.66
Image25.jpg	214.1183	17.1819	750
Image26.jpg	140.4803	8.0168	461.69
Image27.jpg	103.8853	8.9022	380.12
Image28.jpg	83.9656	11.7396	404.10
Image29.jpg	110.7896	9.8877	449.08
Image30.jpg	94.3047	8.6862	335.81
Image31.jpg	163.6936	11.1628	749.09
Image32.jpg	235.1196	29.9839	750
Image33.jpg	242.0532	27.6943	750
Image34.jpg	138.6117	9.5472	542.51
Image35.jpg	138.6117	9.5472	542.51
Image36.jpg	126.6823	9.1701	476.24
Image37.jpg	178.5756	16.3401	750
Image38.jpg	190.2867	9.1504	713.81
Image39.jpg	172.0717	8.6897	612.98
Image40.jpg	144.8953	10.2643	609.70
Image41.jpg	192.1515	10.7010	750
Image42.jpg	162.6694	10.6493	710.16
Image43.jpg	164.1706	10.5294	708.65
Image44.jpg	111.4931	12.5516	573.69
Image45.jpg	157.1099	14.2626	750.00
Image46.jpg	192.8620	9.4070	743.75
Image47.jpg	171.5514	9.3450	657.21
Image48.jpg	243.0895	8.4063	750
Image49.jpg	99.9324	6.4474	264.13
Image50.jpg	110.8008	8.0309	364.78

TABLE II: Thunderstorm Detection

Image No	Experimental Result	Historical Result	Prediction
Image1.jpg	Thunderstorm	No Thunderstorm	False
Image2.jpg	Thunderstorm	Thunderstorm	True
Image3.jpg	Thunderstorm	Thunderstorm	True
Image4.jpg	Thunderstorm	Thunderstorm	True
Image5.jpg	Thunderstorm	Thunderstorm	True
Image6.jpg	Thunderstorm	Thunderstorm	True
Image7.jpg	Thunderstorm	No Thunderstorm	False
Image8.jpg	Thunderstorm	Thunderstorm	True
Image9.jpg	Thunderstorm	Thunderstorm	True
Image10.jpg	Thunderstorm	Thunderstorm	True
Image11.jpg	Thunderstorm	Thunderstorm	True
Image12.jpg	Thunderstorm	Thunderstorm	True
Image13.jpg	Thunderstorm	Thunderstorm	True
Image14.jpg	Thunderstorm	Thunderstorm	True
Image15.jpg	Thunderstorm	Thunderstorm	True
Image16.jpg	Thunderstorm	Thunderstorm	True
Image17.jpg	Thunderstorm	Thunderstorm	True
Image18.jpg	Thunderstorm	No Thunderstorm	False
Image19.jpg	Thunderstorm	Thunderstorm	True
Image20.jpg	Thunderstorm	Thunderstorm	True
Image21.jpg	Thunderstorm	Thunderstorm	True
Image22.jpg	Thunderstorm	Thunderstorm	True
Image23.jpg	Thunderstorm	Thunderstorm	True
Image24.jpg	Thunderstorm	Thunderstorm	True
Image25.jpg	Thunderstorm	No Thunderstorm	False
Image26.jpg	Thunderstorm	Thunderstorm	True
Image27.jpg	Thunderstorm	Thunderstorm	True
Image28.jpg	Thunderstorm	Thunderstorm	True
Image29.jpg	Thunderstorm	Thunderstorm	True
Image30.jpg	No Thunderstorm	Thunderstorm	False
Image31.jpg	Thunderstorm	Thunderstorm	True
Image32.jpg	Thunderstorm	Thunderstorm	True
Image33.jpg	Thunderstorm	Thunderstorm	True
Image34.jpg	Thunderstorm	Thunderstorm	True
Image35.jpg	Thunderstorm	Thunderstorm	True
Image36.jpg	Thunderstorm	Thunderstorm	True
Image37.jpg	Thunderstorm	Thunderstorm	True
Image38.jpg	Thunderstorm	Thunderstorm	True
Image39.jpg	Thunderstorm	Thunderstorm	True
Image40.jpg	Thunderstorm	Thunderstorm	True
Image41.jpg	Thunderstorm	Thunderstorm	True
Image42.jpg	Thunderstorm	Thunderstorm	True
Image43.jpg	Thunderstorm	Thunderstorm	True
Image44.jpg	Thunderstorm	Thunderstorm	True
Image45.jpg	Thunderstorm	Thunderstorm	True
Image46.jpg	Thunderstorm	Thunderstorm	True
Image47.jpg	Thunderstorm	Thunderstorm	True
Image48.jpg	Thunderstorm	Thunderstorm	True
Image49.jpg	No Thunderstorm	No Thunderstorm	True
Image50.jpg	No Thunderstorm	No Thunderstorm	True

The preliminary results presented in Table I and II shows that the wavelength of the thunderstorm image lies is in the range of 380nm-750nm.

Consider an image1.jpg; its calculated wavelength is 409.93nm, which is a presence of thunderstorm. As the predicted experimental result represents thunderstorm and the historical result represent no thunderstorm, this indicates that the prediction is false. Also consider another image7.jpg; its calculated wavelength is 511.28nm, which lies in the range established for the presence of thunderstorm. As the predicted experimental result

represent thunderstorm and the historical cloud image signifies no thunderstorm, this indicates that the prediction is false. Consider an image 18.jpg; its calculated wavelength is 427.18nm, which lie in the established range for the presence of thunderstorm, even the historical data signifies no thunderstorm; this indicates that the prediction is false.

The main goal of the present research is to detect the thunderstorms as accurate as possible. In order to compute accuracy for the present research TP, TN, FP, FN values are to be computed. The true positive (TP) specifies the positive tuples that were correctly labelled. The true negative (TN) specifies the negative tuples that were correctly labelled. The false positive (FP) specifies the negative tuples that are incorrectly labelled. The false negative (FN) specifies the positive tuples that are incorrectly labelled. The four basic performance measures i.e. sensitivity, specificity, accuracy and precision are computed for the present research in order to test how well the proposed system is working and the computations are done by using equation.

Sensitivity, specificity, Accuracy and Precision as well as prediction are expressed as percentages for ease of interpretation. If the sample sizes in the accuracy and the precision groups do not reflect the real value of the thunderstorm, then the accuracy and precision values cannot be estimated and it should ignore those values. Alternatively, when the prevalence is known then the accuracy and precision values can be calculated using the following formula's based on Bays' theorem:

$$\text{Sensitivity} = \frac{TP}{TP + FN}$$

$$\text{Specificity} = \frac{TN}{FP + TN}$$

$$\text{Accuracy} = \frac{TP + TN}{TP + FN + TN + FP}$$

$$\text{Precision} = \frac{TP}{TP + FP}$$

From Table I, II, the performance measures such as sensitivity, specificity, accuracy and precision are calculated using TP, TN, FP and FN and shown in Table III. The proposed method is compared with previous methodologies in the prediction of thunderstorms and is shown in Table IV. The comparison graph is drawn for all the algorithms and is shown in figure 2. The graph clearly shows that the proposed method is outperforming when compared with the previous methodologies

TABLE III: Performance measure for Thunderstorm

Performance Measure	Percentage (%)
Sensitivity	95.56
Specificity	80
Accuracy	94
Precision	91.82

TABLE IV: Accuracy of method with existing methods

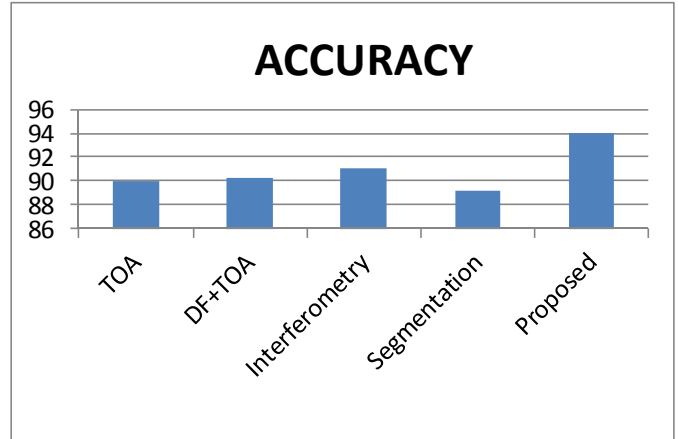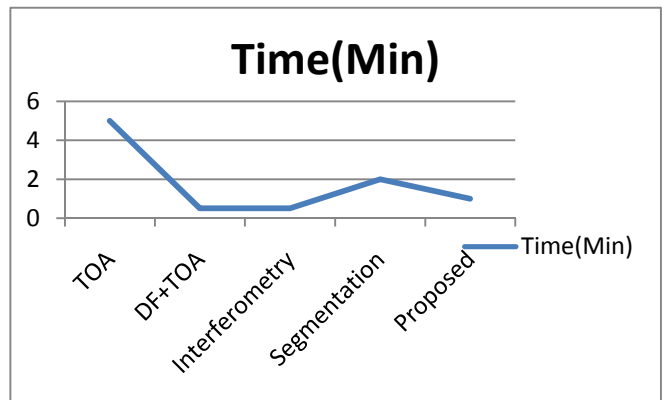| Method	Accuracy	Elapsed time	Revealing
TOA	90.00%	5 min	CG only
DF+TOA	91.28%	~ 30 sec	CG+CC
Interferometry	91%	~ 30 sec	CG+CC
Segmentation	89.2%	2min	CG+CC
Proposed	94%	1min	CG+CC

Figure 2: Comparison graph for proposal method

Figure 3: Elapsed time comparison with existing methods

V. CONCLUSIONS

The aim of the system is to detect the thunderstorm as accurately as possible with in a minimum elapsed time. It has been conducted with k- means clustering technique and Haar wavelet transforms for the prediction of thunderstorms and also adding one more level with saliency map for getting desired portion. A statistical analysis based on threshold value and wavelength range has computed for the detection by using real time satellite imagery. This is conducted to investigate the occurrence of thunderstorms by using wavelet transforms and clustering techniques. It has been outperforming the previous methods such as TOA, DF+TOA, Interferometry, segmentation methods in the detection of thunderstorm. The proposed method predicts the thunderstorms more accurately than the previous method.

REFERENCE

[1] Himadri Chakrabarty, Murthy, C. A., Sonia Bhattacharya and Ashis Das Gupta, "Application of Artificial Neural Network to Predict Squall-Thunderstorms Using RAWIND Data," International Journal of Scientific and Engineering Research, 2013, pp. 1313-1318

[2] Litta, A.J., Sumam Mary Idicula and Naveen Francis C, "Artificial Neural Network Model for the Prediction of Thunderstorms over Kolkata", International Journal of Computer Applications, 2012, pp. 50-55.

[3] Harvey Stern, "Using A Knowledge based System to predict Thunderstorms," Bureau of Meteorology, Australia.

[4] Rudolf kaltenbock, Gerhard Diendorfer and Nikolai Dotzek, "Evaluation of Thunderstorm Indices from ECMWF Analyses, Lightning data and Severe Storm reports," Atmospheric research Journal, Elsevier, 2009, pp. 381-396.

[5] Tajbakhsh, S., Ghafarian, P, and Sahraian, F., "Instability Indicesn and Forecasting Thunderstorms: the case of 30 April 2009," Natural hazards and Earth System Sciences, 2012, pp. 403-413.

[6] Mahesh Anand, s., Ansupa Dashi, Jagadeesh Kumar, Amit Kesarkar, "Prediction and Classification of Thunderstorms using Artificial Neural Network," International journal of Engineering Science and Technology, 2011, pp. 4031-4035.

[7] D.J. Malan, Physics of Lightning, The English Universities Press, Ltd., London, (176 pp.), 1963.

[8] E.T. Pierce, Atmospherics and radio noise, in Lightning, vol. 1: Physics of Lightning, R.H. Golde, ed., (pp. 351-384), 1977.

[9] M.J. Murphy and K.L. Cummins, 2-D and 3-D cloud discharge detection, 1998 Intl. Lightning Detection Conf., Tucson, AZ, Global Atmospherics, Inc., 1998.

[10] D.A. Smith, X.M. Shao, D.N. Holden, C.T. Rhodes, M. Brook, P.R. Krehbiel, M. Stanley, W. Rison, and R.J. Thomas, A distinct class of isolated intracloud lightning discharges and their associated radio emissions, J. Geophys. Res., (104), (4189-4212), 1999.

[11] P. Richard and J. Y. Lojou, Lightning and forecast of intense precipitation, in Proc. of Lightning and Mountains 1997, France: Société des Electriciens et des Electroniciens, (pp. 338–342), 1997.

[12] C. Lennon and L. Maier, Lightning mapping system, in Proc. Int. Aerospace and Ground Conf. on Lightning and Static Electricity, Cocoa Beach, FL,. NASA Conf. Pub. 3106, (II), (pp. 89- 1 – 89-10), 1991.

[13] L. Maier, C. Lennon, T. Britt, and S. Schaefer, Lightning Detection and Ranging (LDAR) system performance analysis, Paper 8.9 in Proc. 6th Conf. on Aviation Weather Systems, Dallas, TX, Amer. Meteorol. Soc., 1995.

[14] http://www.nssl.noaa.gov/education/svrwx101/thunderstorms/types/

[15] http://www.er-emergency.com/technical-bulletin-lightning-damage-assessments-and-consulting-reports

[16] http://www.photolib.noaa.gov/nssl/lightning1.html